

Analysis of Phase Evaluation Algorithms in an Interferometric Method for Static Deformation Measurement

J. Novák

This article describes and analyses an interferometric method for measuring displacements and deformation. The method can be used for a very accurate evaluation of the change in the surface shape of structures used in industry. The paper proposes several multistep phase calculation algorithms and describes an automatic evaluation process using the measurement technique. A complex analysis is also performed of various factors that can have a negative effect on the practical measurement and evaluation process. An analysis is made of the proposed multistep phase calculation algorithms using the proposed error model. It is shown that the resulting phase measurement errors can be effectively reduced by using suitable phase calculation algorithms. The analysis can be applied for a complex comparison of the accuracy and stability of such algorithms.

Keywords: noncontact deformation measurement, phase calculation algorithms, error analysis.

1 Introduction

The interferometric measurement technique known as electro-optic holography [1-5] is a modern noncontact measurement method based on the interference phenomenon [6,7] and phase shifting [1,7,8]. Like other modern non-destructive digital interferometric techniques, this method can be used for very accurate measurement of static and dynamic shape deformation of structures in many areas of industry [9-15]. Subsequent processing of the measured data enables a strain and stress analysis of the structures to be performed [2,16]. In contrast to classical holographic measurement techniques [17], modern optoelectronic array detectors are used for recording the intensity of the interference field, e.g. CCD, together with highly precise phase shifting devices that enable very accurate evaluation of the phase change of the object wave field. This phase change of the object wave field is closely related to changes in the shape of the measured object surface that are caused, for example, by loading of the structure under investigation. Electro-optic holography is an attractive modern method for measuring, displacements and strains in the field of experimental stress analysis. The technique can be used for measuring both optically smooth and rough surfaces during static or dynamic events.

The automatic evaluation process is studied during static displacement measurement, using the electro-optic holographic method to obtain the required measurement accuracy with various types of phase calculation algorithms. Several multistep phase evaluation algorithms are proposed, and a complex analysis is carried out with respect to main factors that influence the measurement and evaluation process in practice [18-21]. This paper proposes a mathematical model for analysing the main measurement factors. This model enables an analysis of the accuracy and stability of the proposed phase evaluation algorithms with respect to chosen parameters of the affecting factors. An analysis is performed of several phase calculation algorithms using this model. It is shown that the influence of various measurement errors can be effectively reduced by a suitable choice of phase measuring

algorithms. The analysis can be used for a general comparison of any phase evaluation algorithm in phase shifting.

2 Principle of the measurement method

The method uses the interaction of arbitrary coherent wave fields with the tested object in order to determine the change in the shape of the object. Information about the displacement of the object surface is then coded into the phase of the object field, the physical properties of which are modified after reflection from the tested object. To determine this phase we allow the object wave field to interfere with the reference wave field. From the measured values of the recorded intensity of the interference field we are able to obtain phase values. Consider now for simplicity two linearly polarized coherent wave fields with the same polarization vector. Then for the resulting intensity of the interference field in the plane (x,y) of the detector for two different states of the tested object we obtain [5,6]

$$I_i(x, y) = A(x, y) + B(x, y) \cos[\varphi(x, y) + \Psi_i], \quad (1)$$

$$I_{zi}(x, y) = A(x, y) + B(x, y) \cos[\varphi(x, y) + \Psi_i + \Delta\varphi(x, y)], \quad (2)$$

where A and B are functions that characterize the mean intensity and modulation of the recorded interference signal, φ is the phase difference between the object and the reference field, I_i and I_{zi} are the values of the intensity in the i -th frame with phase shift Ψ_i , $\Delta\varphi$ is the change of the phase of the object field. It is necessary to capture at least three phase-shifted interferograms to determine phase values $\Delta\varphi$ unambiguously with the phase shifting technique [1,7].

For static measurements, N phase-shifted interference patterns are recorded in two different states of the investigated object, e.g. in different loading states. In the general case we can derive the following equation for the phase change $\Delta\varphi$ of the object wave field at some point (x,y)

$$\tan[\Delta\varphi(x, y)] = \frac{\sum_{j=1}^N \sum_{i=1}^N I_{zj}(x, y) I_i(x, y) [C_i D_j - C_j D_i]}{\sum_{j=1}^N \sum_{i=1}^N I_{zj}(x, y) I_i(x, y) [C_i C_j - D_i D_j]}, \quad (3)$$

where

$$C_i = Q_{11} + Q_{12} \cos \Psi_i + Q_{13} \sin \Psi_i \quad (4a)$$

$$D_i = Q_{21} + Q_{22} \cos \Psi_i + Q_{23} \sin \Psi_i \quad (4b)$$

and N is the number of phase shifted intensity measurements and Ψ_i is the phase shift. The quantities Q_{kl} can be expressed from

$$\begin{aligned} Q_{11} &= g_{12}g_{23} - g_{13}g_{22}, & Q_{12} &= g_{12}g_{13} - g_{11}g_{23}, \\ Q_{13} &= g_{11}g_{22} - g_{12}^2, & & \end{aligned} \quad (5)$$

$$Q_{21} = g_{12}g_{33} - g_{13}g_{23}, \quad Q_{22} = g_{13}^2 - g_{11}g_{33},$$

$$Q_{23} = g_{11}g_{23} - g_{12}g_{13}.$$

where the matrix \mathbf{G} is given by

$$\mathbf{G} = \begin{pmatrix} g_{11} & g_{12} & g_{13} \\ g_{12} & g_{22} & g_{23} \\ g_{13} & g_{23} & g_{33} \end{pmatrix} = \begin{pmatrix} N & \sum \cos \Psi_i & \sum \sin \Psi_i \\ \sum \cos \Psi_i & \sum \cos^2 \Psi_i & \sum \cos \Psi_i \sin \Psi_i \\ \sum \sin \Psi_i & \sum \cos \Psi_i \sin \Psi_i & \sum \sin^2 \Psi_i \end{pmatrix}. \quad (6)$$

Equation (3) is a general phase calculation algorithm. The calculated phase values $\Delta\varphi$ are located in the range $[-\pi, \pi]$. The discontinuous distribution of the evaluated phase values, so called wrapped phase values, must be reconstructed (unwrapped) using suitable mathematical techniques [23,24]. The unwrapped phase values $\Delta\varphi$ are then closely related to the optical path difference between the object and reference

beam and subsequently also to the displacement of the object surface. This relation can be expressed for any observed point P on the object surface as

$$\Delta\varphi(P) = \frac{2\pi}{\lambda} W(P) = \mathbf{s}(P) \mathbf{d}(P), \quad (7)$$

where $\Delta\varphi$ is the phase change of the object wave field for two different states of the object, λ is the wavelength of light, \mathbf{d} is the displacement vector, and \mathbf{s} is the sensitivity vector. The sensitivity vector is defined as [2]

$$\mathbf{s}(P) = \frac{2\pi}{\lambda} [\mathbf{a}(P) - \mathbf{b}(P)], \quad (8)$$

where \mathbf{a} is the illumination direction and \mathbf{b} is the observation direction. The displacement vector \mathbf{d} can be determined from (7) [25]. The principal scheme for measurement of displacements is shown in Fig. 1.

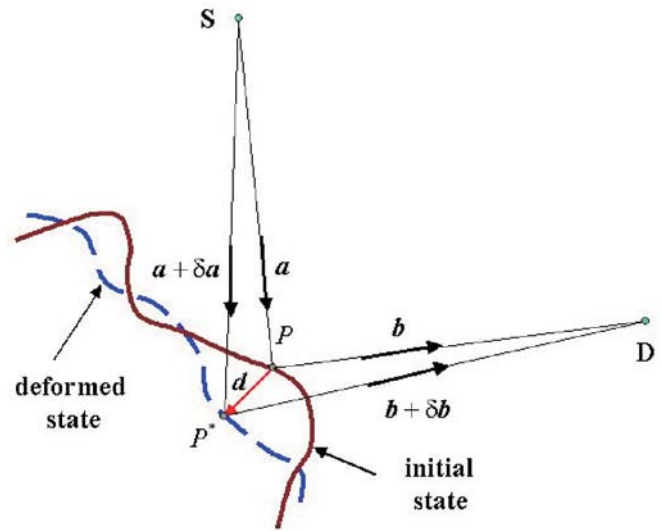


Fig. 1: Measurement of displacements

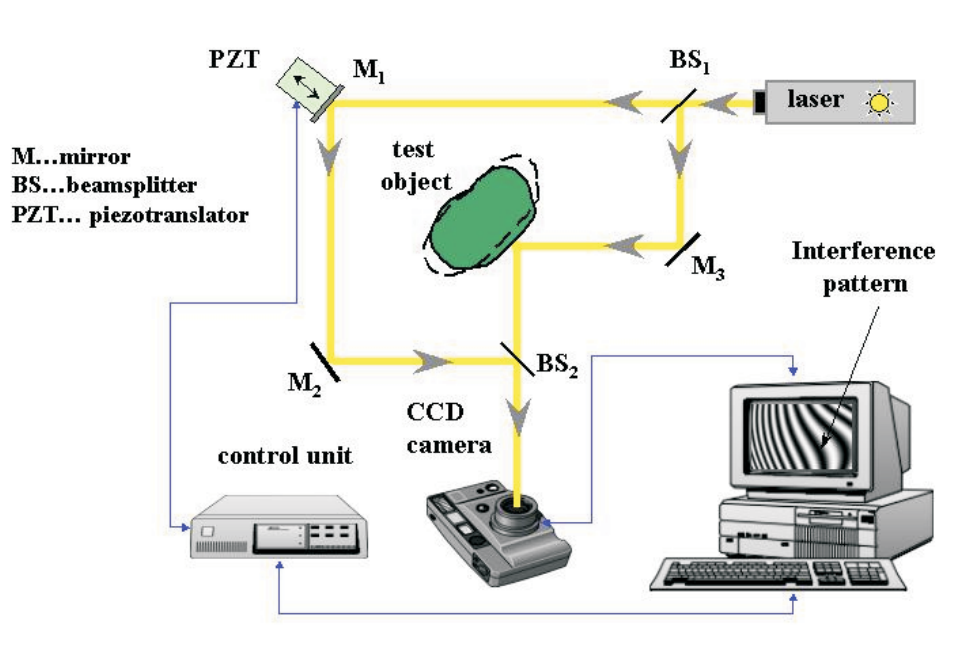


Fig. 2: Experimental scheme of the measurement system

3 Experimental arrangement for deformation measurement

We now focus on practical implementation of the described measurement technique for measuring the change in the shape of the measured object. Figure 2 shows an experimental scheme of the measurement system with a piezotranslator used as a phase shifting device. Phase shifting is implemented into the reference beam by shifting a small plane mirror M_1 mounted on a very precise piezoelectric transducer PZT. The beam of light from the source of coherent radiation (laser) is divided into two beams by the beamsplitter BS_1 . The first beam (reference beam) reflects successively from mirror M_1 , mirror M_2 and beamsplitter BS_2 . The second beam (object beam) reflects from mirror M_3 and test object O . Then the object beam passes through beamsplitter BS_2 . Both beams (reference and object) interfere, and the CCD sensor detects the resulting intensity of the interference field in a chosen plane (x,y) . The main element in the whole experimental measuring system is the computer with the control unit, which controls the precise shifting of the piezotranslator and detection of the intensity of the light with a CCD sensor.

4 Analysis of the Measurement and Phase Evaluation Process

The overall accuracy of interferometric measuring techniques is expressed in terms of systematic and random errors during the measurement process. There are many factors that can influence the measurement accuracy. The sensitivity of phase calculation with respect to parameters A , B and ψ in the interference equation (2) depends on the specific phase measuring algorithm used for measurement evaluation. Gen-

erally, errors in interferometric measurements can be classified into two distinct categories: *systematic* and *random* errors. In order to identify the parameters which introduce errors into the measurement and evaluation process the different components of the interferometric system are considered (see Table 1). In practice, some of these errors can be avoided in advance, e.g. by proper choice of components of the measuring system. The most important types of errors in the described measuring technique are random and systematic errors caused by the phase shifting device and by the detector.

A very interesting and important task for practical use of the method is to find out the accuracy of the method for a given measurement arrangement. In the case of small changes in $\Delta\varphi$ the error of the phase difference $\Delta\varphi$ can be expressed as

$$\delta(\Delta\varphi) = \cos^2 \Delta\varphi [\delta(\tan\Delta\varphi)], \quad (9)$$

where function $\delta(\tan\Delta\varphi)$ depends on the values of the intensity detection error, the phase shift error and the form of the particular evaluation algorithm.

Functions $\tan\Delta\varphi$ can be derived for different values of the phase shift ψ from (3). In our work, a numerical model was proposed for determining the influence of the most important measurement factors on the phase evaluation process. A study was made of the impact on the overall accuracy and stability of the phase evaluation algorithms in this method. Random and systematic errors of the phase shifting device and the detector were simulated with a computer program and the resulting phase error was determined. It was assumed that the random errors behave as normally distributed quantities with the mean value zero. The error of the phase shifting device can be modelled by the expression [19, 26]

Table 1

Parameters	Error origin	Classification
Laser	Variation of mean intensity	Systematic
	Variation of coherence	Systematic
	Variation of laser frequency	Systematic
	Photon noise	Random
Phase shifting device	Miscalibration of phase shift	Systematic
	Non-linearity of phase shift	Systematic
	Inequality of phase shift	Random
Detector	Electronic noise	Random
	Quantization noise	Random
	Non-linear detection	Systematic
Optical parts	Geometrical aberrations	Systematic
Environmental parameters	Vibrations	Random
	Fluctuations of refractive index	Random
Sensitivity of the measuring system	Improper arrangement of the measurement system	Systematic

$$\delta\Psi_i = \Psi_i \sum_{k=0}^{\infty} c_{k+1} \left(\frac{\Psi_i}{2\pi}\right)^k + \sigma_{\Psi}, \quad (10)$$

where ψ_i is the phase shift, c_k are coefficients of systematic errors of the phase shifting device, and σ_{Ψ} is the random error of the phase shifting device. Coefficients c_k describe the real (nonlinear) behaviour of the chosen phase shifting device. However, the first two coefficients c_1 and c_2 are most significant for the measurement and evaluation process in practice. The standard deviation of the random error distribution can be determined for our model from the accuracy of the phase shifting device. Assume now that we use a very precise piezoelectric translator for phase shifting. The non-linearity is then in the range 0.01–0.2% and the repeatability of the shifting is $\pm(1-10)$ nm [27]. From the repeatability of the phase shifting device we can calculate the corresponding phase change from the relation

$$\delta\varphi = \frac{2\pi}{\lambda} \delta W, \quad (11)$$

where δW is the change of the optical path difference caused by shifting a small mirror in the path of the reference beam, and λ is the wavelength of light. In the case of a He-Ne laser with the wavelength $\lambda = 632.8$ nm, the phase error will be approximately in the range 0.2–0.01 radians. The error in detection of the intensity of the observed interference field can be modelled on the basis of

$$\delta I = I \sum_{k=1}^{\infty} d_k I^k + \sigma_I, \quad (12)$$

where I is the intensity of the interference field, d_k are coefficients that characterize the systematic errors in intensity detection, and σ_I is the random error in intensity detection. Coefficients d_k describe the real (nonlinear) behaviour of the given detector of the intensity of the interference field. The most important factor for a real description of the detector response on the incident light is coefficient d_1 , which describes the second order non-linear response of the detector. The standard deviation that characterizes the distribution of random errors during the detection process of the interference signal can be simulated as a fraction of the intensity incident onto the detector, i.e. $\sigma_I = pI$, where values of p can be considered in the range 0.1–1% with respect to the properties of the currently produced detectors used for recording the intensity of the interference field.

It is important to know which properties of the individual elements of the measurement system are needed in order to obtain the required accuracy of the calculated phase values using some of the phase calculation algorithms. These factors were implemented into a numerical model that can simulate the impact on the measurement accuracy of the individual parameters that describe these factors [20]. The model of the intensity distribution for the i -th measurement can be expressed as

$$I_i = A + B \cos[\Delta\varphi + \Psi_i + \delta\Psi_i] + \delta I, \quad (13a)$$

$$A = (I_0 + I_R), \quad B = 2\sqrt{I_0 I_R}, \quad (13b)$$

where I_R is the intensity of the reference beam, I_0 is the intensity of the object beam, A is the mean intensity of the interference signal, B is the modulation of the interference

signal, $\Delta\varphi$ is the phase change of the object beam, ψ_i is the phase shift in i -th intensity measurement, $\delta\psi_i$ is the phase shift error, and δI is the detection error. The resulting error of phase values $\Delta\varphi$ is then given by

$$\delta(\Delta\varphi) = \Delta\varphi' - \Delta\varphi, \quad (14)$$

where $\Delta\varphi'$ are the calculated phase values and $\Delta\varphi$ are the original phase values. For the performed error analysis values $\Delta\varphi$ were considered in the range $(-\pi, \pi)$. Now we can study the influence of the described factors on the accuracy of phase calculation for individual phase measuring algorithms in electro-optic holography. A root-mean-square $\sigma_{\Delta\varphi}$ of calculated phase errors was chosen as an error characteristic, i.e.

$$\sigma_{\Delta\varphi} = \sqrt{\sum_{i=1}^M \delta(\Delta\varphi)_i^2} / M, \quad (15)$$

where M is the number of computer simulations of a phase evaluation. More than 500 simulation cycles were performed to guarantee the reliability of the results. The parameters considered in the error analysis of the phase calculation algorithms are shown in Table 2.

Table 2

Coefficient	Value	Units
c_1	1	%
c_2	0.1	%
σ_{Ψ}	0.05	rad
d_1	1	%
p	1	%

From (3) we can derive many phase calculation algorithms by a suitable choice of phase shift values ψ and the number of recorded intensity frames N needed for calculation. In identical measurement conditions, i.e. with the same error factors, the algorithms will differ in their sensitivity to these factors. The following text describes several phase calculation algorithms for electro-optic holography and these algorithms are compared using our model. For simplification of description, the differences between the different intensity measurements were denoted as

$$a_{i,k} = I_i - I_k, \quad b_{i,k} = I_{zi} - I_{zk}, \quad (16)$$

where I_i and I_{zi} are the i -th intensity measurements in two different states of the observed object. I_i and I_{zi} are functions of the phase shift ψ_i in the i -th measurement of the intensity of the interference field. The derived phase calculation algorithms are shown in Table 3. They were denoted as A1–A9.

Figure 3 shows the relationship between the error of phase values $\delta(\Delta\varphi)$ and phase values $\Delta\varphi$ from the range $(-\pi, \pi)$, which enables a comparison of the accuracy and stability of the phase calculation algorithms.

We can observe that the resulting phase error $\delta(\Delta\varphi)$ is very dependent on phase values $\Delta\varphi$, and the algorithms differ in the accuracy and stability of phase calculation in the given range. With increasing number of steps N the phase error decreases, but the phase error also depends on the properties of

Table 3

A1: $N = 3, \Psi = \pi/4$

$$\tan \Delta\varphi = \frac{a_{1,2}b_{3,2} - a_{3,2}b_{1,2}}{a_{1,2}b_{1,2} + a_{3,2}b_{3,2}}$$

A2: $N = 3, \Psi = \pi/2$

$$\tan \Delta\varphi = \frac{a_{1,3}(b_{2,3} - b_{1,2}) - b_{1,3}(a_{2,3} - a_{1,2})}{a_{1,3}b_{1,3} + (a_{2,3} - a_{1,2})(b_{2,3} - b_{1,2})}$$

A3: $N = 3, \Psi = 2\pi/3$

$$\tan \Delta\varphi = \frac{\sqrt{3}[a_{3,2}(b_{1,2} + b_{1,3}) - b_{3,2}(a_{1,2} + a_{1,3})]}{3a_{3,2}b_{3,2} + (a_{1,2} + a_{1,3})(b_{1,2} + b_{1,3})}$$

A4: $N = 5, \Psi = \pi/2$

$$\tan \Delta\varphi = \frac{2b_{2,4}(a_{3,1} + a_{3,5}) - a_{2,4}(b_{3,1} + b_{3,5})}{(a_{3,1} + a_{3,5})(b_{3,1} + b_{3,5}) + 4a_{2,4}b_{2,4}}$$

A5: $N = 5, \Psi = \pi/2$

$$\tan \Delta\varphi = \frac{7[a_{4,2}(3b_{1,3} + 3b_{5,3} + b_{1,2} + b_{5,4}) - b_{4,2}(3a_{1,3} + 3a_{5,3} + a_{1,2} + a_{5,4})]}{49a_{4,2}b_{4,2} + (3a_{1,3} + 3a_{5,3} + a_{1,2} + a_{5,4})(3b_{1,3} + 3b_{5,3} + b_{1,2} + b_{5,4})}$$

A6: $N = 7, \Psi = \pi/2$

$$\tan \Delta\varphi = \frac{(7b_{3,5} - b_{1,7})(4a_{4,2} + 4a_{4,6}) - (7a_{3,5} - a_{1,7})(4b_{4,2} + 4b_{4,6})}{(4a_{4,2} + 4a_{4,6})(4b_{4,2} + 4b_{4,6}) + (7a_{3,5} - a_{1,7})(7b_{3,5} - b_{1,7})}$$

A7: $N = 7, \Psi = \pi/3$

$$\tan \Delta\varphi = \frac{\sqrt{3}[(a_{6,2} + a_{5,3})(b_{1,3} + b_{2,4} + b_{6,4} + b_{7,5}) - (b_{6,2} + b_{5,3})(a_{1,3} + a_{2,4} + a_{6,4} + a_{7,5})]}{3(a_{6,2} + a_{5,3})(b_{6,2} + b_{5,3}) + (a_{1,3} + a_{2,4} + a_{6,4} + a_{7,5})(b_{1,3} + b_{2,4} + b_{6,4} + b_{7,5})}$$

A8: $N = 9, \Psi = \pi/4$

$$\tan \Delta\varphi = \frac{(b_{2,8} + 2b_{3,7} + b_{4,6})(a_{4,1} + a_{5,2} + a_{5,8} + a_{6,9}) - (a_{2,8} + 2a_{3,7} + a_{4,6})(b_{4,1} + b_{5,2} + b_{5,8} + b_{6,9})}{(a_{2,8} + 2a_{3,7} + a_{4,6})(b_{2,8} + 2b_{3,7} + b_{4,6}) + (a_{4,1} + a_{5,2} + a_{5,8} + a_{6,9})(b_{4,1} + b_{5,2} + b_{5,8} + b_{6,9})}$$

A9: $N = 11, \Psi = \pi/2$

$$\tan \Delta\varphi = \frac{4(b_{1,11} + 8b_{9,3} + 15b_{5,7})(a_{2,4} + a_{10,8} + 2(a_{6,4} + a_{6,8})) - 4(a_{1,11} + 8a_{9,3} + 15a_{5,7})(b_{2,4} + b_{10,8} + 2(b_{6,4} + b_{6,8}))}{(a_{1,11} + 8a_{9,3} + 15a_{5,7})(b_{1,11} + 8b_{9,3} + 15b_{5,7}) + 16(a_{2,4} + a_{10,8} + 2(a_{6,4} + a_{6,8}))(b_{2,4} + b_{10,8} + 2(b_{6,4} + b_{6,8}))}$$

the particular algorithm, not only on the number of steps. On the basis of this error analysis we can conclude that the most accurate algorithms are multi-step algorithms A7, A8 and A11. The five-step algorithm also seems to have relatively very good properties as regards measurement errors. However, the three-step phase calculation algorithms A1 and A2 are the least accurate and least stable of all compared algorithms. The third three-step algorithm A3 is evidently rather more accurate than the other three-step algorithms.

From a practical viewpoint, the time needed for the measurement and its automatic evaluation is also important.

Therefore the time for phase calculation using various phase evaluation algorithms was also determined. Table 4 shows the relative computing time, which is taken as the ratio of the computing time for a given algorithm and the minimum computing time for all the algorithms. The computing time was obtained using the computer simulation of phase evaluation with different phase calculation algorithms. It is reasonable to assume that phase calculation algorithms with a larger number of steps N are more time consuming, but on the basis of our analysis we can see that the increase in computing time is not very rapid. The difference in computing time between

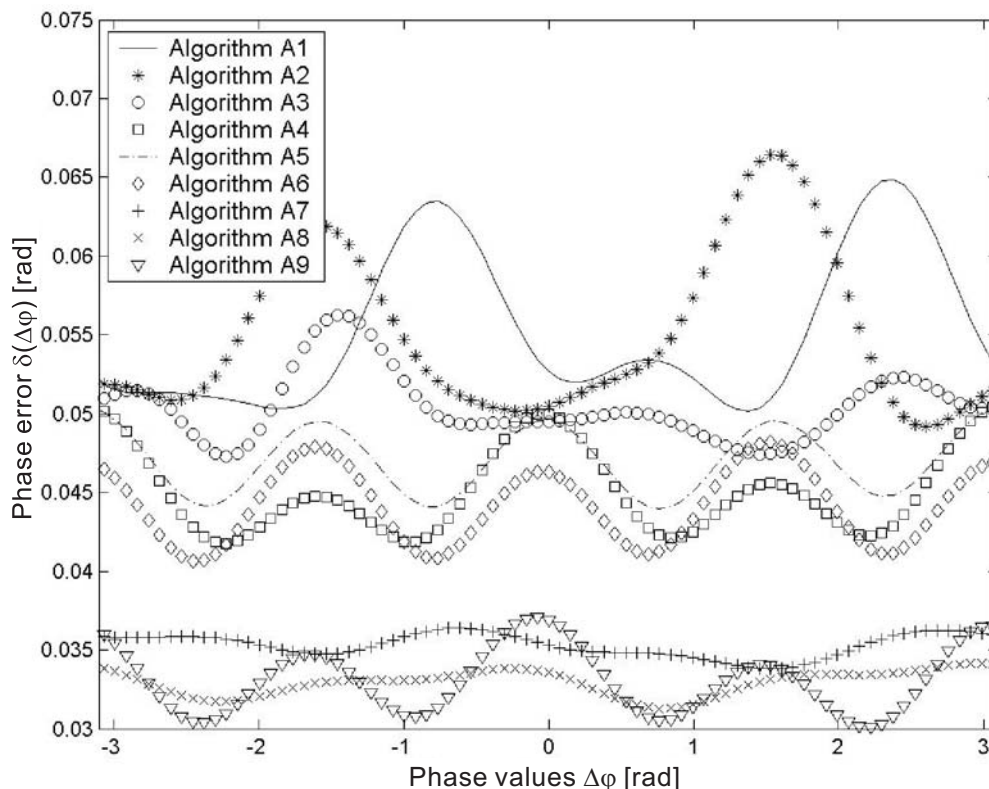


Fig. 3: Relationship between phase error $\delta(\Delta\varphi)$ and phase values $\Delta\varphi$

the fastest three-step and the slowest eleven-step algorithm is approximately 25 %.

It can also be seen that the computing time does not depend directly on the increasing number of steps N . For example, the computing time for algorithms A1, A2 and A4, which differ in the number of steps required for phase evaluation, is practically the same. In order to determine the computing time it is necessary to consider the number of mathematical operations needed for phase calculation with each particular algorithm. However, it should be noted that the time for the phase shifting process itself, i.e. shifting the piezotranslator between individual captured intensity frames, needs to be included in the total time for phase evaluation.

Table 4

Algorithm	Relative computing time [%]
A1	100
A2	105
A3	110
A4	104
A5	118
A6	116
A7	121
A8	120
A9	128

If we try to summarize the results of the performed analysis, it will in most cases in practice be sufficient to use five-step phase calculation algorithms, which are very accurate and less time consuming. To obtain greater measurement accuracy, algorithms with a larger number of steps can be used, but the practical application of phase calculation algorithms with a greater number of intensity measurements depends on the specific character of the measurement. These algorithms need a longer time to record all frames, which may not satisfy the requirements for the measurement, e.g. in the case of a measurement in an environment with quickly changing thermo-mechanical parameters.

5 Conclusion

We have described a noncontact interferometric measurement technique that can be used for deformation measurement in industry. The method is based on the principle of interference of arbitrary coherent wave fields and the phase shifting technique for automatic analysis of a measurement in real time. It can be used for very precise testing of various types of structures and objects in science and engineering. In order to detect the interference field, modern optoelectronic elements are used together with computers. This enables the measurement analysis to be carried out automatically in real time using suitable phase calculation algorithms. A general equation for phase evaluation was described, and several phase calculation algorithms were derived. Complex error analysis was performed on them. The influence of the main factors that affect the accuracy of phase evaluation was considered in the error analysis. It is shown that phase measurement errors can be decreased by a proper choice of the phase calcu-

lation algorithm. The analysis can be applied for comparing any phase measurement algorithms.

Acknowledgement

This work was supported by grant No. 103/03/P001 of the Grant Agency of the Czech Republic.

References

- [1] Malacara, D.: *Optical shop testing*. New York: John Wiley & Sons, 1992.
- [2] Kreis, T.: *Holographic interferometry: Principles and methods*. Berlin, Akademie Verlag 1996.
- [3] Stetson, K. A.: *Electro-optic holography and its application to hologram interferometry*. Applied Optics, 1985, Vol. 24, No. 21, p. 3631.
- [4] Stetson, K. A., Brohinsky, W. R.: *Electro-optic holography system for vibration analysis and non-destructive testing*. Optical Engineering, 1987, Vol. 26, No. 12, p. 1234.
- [5] Miks, A.: *Applied optics 10* (in Czech), Prague: CTU Publishing House, 2000.
- [6] Born, M., Wolf, E.: *Principles of optics*. 6th ed. New York: Pergamon Press, 1980.
- [7] Creath, K.: *Phase-measurement interferometry techniques*. Progress in optics Vol. XXVI, Amsterdam: Elsevier Science, 1988.
- [8] Robinson, D. W., Reid, G. T.: *Interferogram analysis: Digital fringe pattern measurement Techniques*. Bristol: Institute of Physics Publishing, 1993.
- [9] Rastogi, P. K.: *Digital speckle pattern interferometry and related techniques*. New York: John Wiley & Sons, 2001.
- [10] Cloud, G.: *Optical methods of engineering analysis*. Cambridge: Cambridge Univ. Press, 1998.
- [11] Rastogi, P. K.: *Handbook of optical metrology*. Boston: Artech House Publishing, 1997.
- [12] Jacquot, P., Fournier, J. M., (ed.): *Interferometry in speckle light: Theory and applications*. Berlin: Springer Verlag, 2000.
- [13] Osten, W., Jüptner, W., (ed.): *Fringe 2001: The 4th international workshop on automatic processing of fringe patterns*. Paris, Elsevier, 2001.
- [14] Osten, W., Jüptner, W., Kujawinska, M. (ed.): *Optical measurement systems for industrial inspection II*. SPIE Proceedings Vol. 4398, Washington: SPIE 2001.
- [15] Rastogi, P. K., Inaudi, D.: *Trends in optical non-destructive testing and inspection*. Amsterdam: Elsevier, 2000.
- [16] Kobayashi, A. S. (ed.): *Handbook of experimental mechanics*. New Jersey: Prentice Hall, 1987.
- [17] Vest, Ch. M.: *Holographic interferometry*. New York: John Wiley & Sons, 1979.
- [18] Miks, A., Novak, J.: *Non-contact measurement of static deformations in civil engineering*. Proceedings of ODIMAP III: Optoelectronic Distance/Displacement Measurements and Applications, Pavia: University of Pavia, 2001, p. 57–62.
- [19] Novak, J.: *Computer simulation of phase evaluation process with phase shifting technique*. Physical and material engineering 2002, Prague: CTU, 2002, p. 87–88.
- [20] Novak, J.: *Error analysis of three-frame algorithms for evaluation of deformations*. Interferometry of speckle light: Theory and applications, Berlin: Springer Verlag, 2000, p. 439–444.
- [21] Miks, A., Novak, J.: *Application of multi-step algorithms for deformation measurement*. SPIE Proceedings Vol. 4398, Washington: SPIE, 2001, p. 280–288.
- [22] Novak, J.: *Error analysis for deformation measurement with electro-optic holography*. Fine mechanics and optics, Vol. 6, 2000, p. 166.
- [23] Ghiglia, D. C., Pritt, M. D.: *Two-dimensional phase unwrapping: Theory, algorithms and software*. New York: John Wiley & Sons, 1998.
- [24] Novák, J.: *Methods for 2-D phase unwrapping*. In MATLAB 2001 Proceedings, Prague: VŠCHT Publishing House, 2001.
- [25] Stetson, K. A.: *Use of sensitivity vector variations to determine absolute displacements in double exposure hologram interferometry*. Applied Optics, 1990, Vol. 29, No. 4, p. 502.
- [26] Zhang, H., Lalor, M. J., Burton, D. R.: *Error-compensating algorithms in phase-shifting interferometry: a comparison by error analysis*. Optics and Lasers in Engineering, 1999, Vol. 31, p. 381.
- [27] *Physik Instruments catalogue 2002*.

Ing. Jiří Novák, Ph.D.
 phone1: +420 224 354 435
 fax: +420 233 333 226
 e-mail: novakji@fsv.cvut.cz

Department of Physics
 Czech Technical University in Prague
 Faculty of Civil Engineering
 Thákurova 7
 166 29 Prague 6, Czech Republic